Journal of Computing and Electronic Information Management
ISSN: 2413-1660 | Vol. 13, No. 3, 2024

Numerical Analysis Of Natural Convection In A Closed Circular Cavity With A Elliptical Heater

Ting Zheng [1,2]

[1] College of Intelligent Manufacturing and Automotive Engineering, Luzhou Vocational & Technical College, Luzhou 646000, China
[2] Intelligent Manufacturing Luzhou Key Laboratory, Luzhou Vocational & Technical College, Luzhou 646000, China

Abstract: The natural convection heat transfer in a closed circular cavity containing a constant temperature elliptic heating body was studied by finite volume method. The influences of Rayleigh number Ra, relative size of heating element and rotation Angle on flow and heat transfer in the cavity are discussed. The variation range of Rayleigh number is 103 ~ 106, the variation range of length-diameter ratio of elliptic long axis to cavity diameter is 0.1 ~ 0.4, and the variation range of rotation angle is 0° ~ 90°.The results show that the changes of the above three parameters can affect the structure of temperature field and flow field in the cavity. Increasing the Rayleigh number, decreasing the size of the heating element and increasing the rotation Angle of the heating element will be more conducive to the heat transfer in the cavity. The research results can provide theoretical basis for the heat dissipation and management of electronic equipment.

Keywords: Natural convection; Closed circular cavity; Elliptic heater; Length-diameter ratio; Rotation angle.

1. Introduction

The study of natural convection in closed chambers has a wide range of applications in many fields, such as the management of safety systems in nuclear reactors, the growth of crystals, the heating of buildings and the dissipation of heat from electronic devices. Natural convection in closed cavities with built-in heat emitters is affected by the structure of the cavity, the shape and size of the heat source, and the location of the heat transfer. Cavity structure commonly used in engineering is mainly square, and the shape of the built-in heat generator is mainly square and round, considering the actual engineering applications, more complex cavity and heat generator shapes may appear, in order to get a better heat transfer effect, the natural convection in a circular closed cavity with a built-in ellipsoidal heat generator has a research value.

Natural convection in closed cavities without built-in heat sources has been investigated by many scholars[1-4] . On this basis, the literature[5-9] based on the literature, the natural convection in a square cavity with a circular heat generator has been investigated by numerical simulation. Liao, C C[10] et al. studied the natural convection in a closed square cavity with built-in heaters of different shapes, and the results showed that the ellipsoidal heaters have larger local and average Nusselt numbers than the circular heaters, but the heat transfer capacity of the corresponding cavities decreases. Ping, Zhang[11] et al. investigated the natural convection in a closed square cavity containing a separate elliptical heat emitter, and showed that the heat transfer capacity in the square cavity is enhanced with the increase of the Rayleigh number, while it has little relationship with the rotation angle of the square cavity. Wang Rui[12] et al. obtained the natural convection in a triangular closed cavity with an inner square heat generator through numerical simulation, and found that the two right-angled edges of the triangular cavity with smaller aspect ratio are more favourable to the air flow, which has a better heat exchange effect.[13] et al. investigated the natural convection in a triangular cavity with a circular heater, and found that for a triangular cavity, increasing the size of the built-in circular heater is more conducive to heat transfer in the cavity.

2. Physical modelling

The geometrical model studied in this paper is shown in Figure. 1. Where the closed cavity is a circle with a diameter of D, built-in concentric elliptical heat generator, the ellipse long and short axes are m, n, respectively, the value of m is taken as 0.1D, 0.2D, 0.3D and 0.4D, respectively, and m=2n, and the heat generator is rotated around the centre of the circle by 30 °, 60 °, and 90 °, respectively. The surface of the circular cavity is a constant temperature cold wall surface with temperature Tc and the surface of the heat generator is a constant temperature hot wall surface with temperature Th and ΔT=40K . The coordinate origin is located at the centre of the cavity, the direction of gravity is the negative direction of the y-axis, and the medium between the heat generator and the cavity is air.

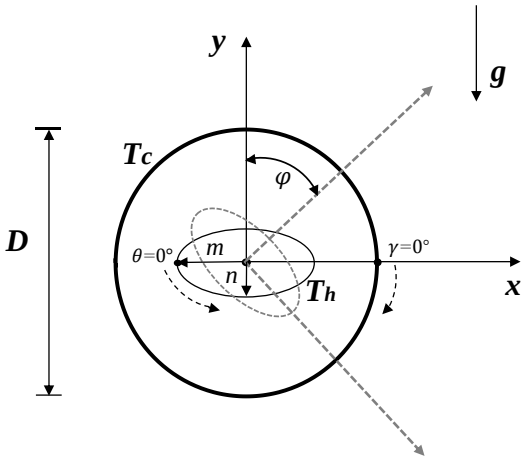

Fig.1 Schematic diagram of physical model and reference coordinate system

Due to the small temperature difference of the computational model in this paper, the air medium is usually treated with the Boussinesq assumption, ignoring the viscous

thermal effect and assuming that all other physical parameters are constants. The flow pattern of the air medium in the cavity is judged according to Table I. The Rayleigh number in this paper is studied in the range of 103 ~ 106, so it is set as a stable laminar flow. On this basis, the influence of radiation and thermal conductivity of the cavity and the wall surface of the heat generator, as well as the influence of other factors on the natural convection in the cavity are not considered.

Table. 1 Criterion of flow pattern

Stratified flow	Transition flow	Turbulent flow
$Ra < 10^8$	$10^8 < Ra < 10^{10}$	$10^{10} < Ra$

3. Numerical techniques

Based on the Boussinesq assumption, the following control equations (1) to (4) are obtained according to the coordinate system established in Figure. 1

Continuity equations:

$$\frac{\partial U}{\partial X}+\frac{\partial V}{\partial Y}=0 \tag{1}$$

Momentum equation in the x-axis direction:

$$U\frac{\partial U}{\partial X}+V\frac{\partial U}{\partial Y}=-\frac{\partial P}{\partial X}+\frac{\partial^2 U}{\partial X^2}+\frac{\partial^2 U}{\partial Y^2} \tag{2}$$

Y-axis direction momentum equation:

$$U\frac{\partial V}{\partial X}+V\frac{\partial V}{\partial Y}=-\frac{\partial P}{\partial Y}+\frac{\partial^2 V}{\partial X^2}+\frac{\partial^2 V}{\partial Y^2}+\left(\frac{Ra}{Pr}\right)\Phi \tag{3}$$

The energy equation:

$$U\frac{\partial \Phi}{\partial X}+V\frac{\partial \Phi}{\partial Y}=\frac{1}{Pr}\left(\frac{\partial^2 \Phi}{\partial X^2}+\frac{\partial^2 \Phi}{\partial Y^2}\right) \tag{4}$$

The dimensionless parameters are defined as follows:

$$X=\frac{x}{D},\ Y=\frac{y}{D},\ U=\frac{uD}{\nu},\ V=\frac{vD}{\nu},\quad \Phi=\frac{T-T_c}{T_h-T_c},\ P=\frac{(p+\rho gy)D^2}{\rho\nu^2} \tag{5}$$

where u and v are the velocity components in the x and y directions respectively, p is the pressure, ρ is the density, and ν is the kinematic viscosity.

As shown in equation (6), Rayleigh number and Planck number are two dimensionless parameters of fluid mechanics and heat transfer, Rayleigh number is an important parameter characterize the intensity of convective heat transfer inside the closed cavity, and Planck number is a parameter characterize the relative relationship between fluid momentum exchange and heat exchange. Since the cavity medium is air, the Platt's number is set to 0.71; the wall surface of the heat generator is the thermostatic hot wall surface Φ=1, the wall surface of the cavity is the thermostatic cold wall surface Φ=0, and the two wall surfaces are all fixed without sliding wall surface U=V=0. Among them, β is the thermal expansion coefficient and α is the thermal diffusion coefficient.

$$Ra=\frac{g\beta\Delta TD^3}{\nu\alpha},\ Pr=\frac{\nu}{\alpha} \tag{6}$$

Localized surface Nussle number versus average surface Nussle number:

$$Nu=\left.\frac{\partial\Phi}{\partial n}\right|_{wall},\ Nu_{ave}=\frac{1}{S}\int_0^s\frac{\partial\Phi}{\partial n}dS \tag{7}$$

4. Computational validation of the model

A double precision 2ddp unsteady pressure basis implicit solution was chosen, using the SIMPLE algorithm for velocity and pressure, PRESTO and QUICK for pressure and momentum discretisation formats, respectively, and the second order windward format energy equation. Convergence is considered to be reached with momentum residuals of 10-3, and energy residuals of 10-6.

In order to verify the accuracy of the calculation model, it is necessary to verify the independence of the calculation grid, select the Rayleigh number of 104 , the long axis of the heating body m = 0.2D, the rotation angle , respectively, divided into the number of grids of 5400, 7600, 10500, 14900, found that as the number of grids increases, the average Nussle number of the surface of the heating body has very little change, when the number of grids is greater than 10050, its value is basically unchanged, in order to calculate the accuracy as well as the time spent on the consideration, the number of grids of 10500 is chosen to calculate.

Since there is no physical model consistent with this paper as a reference, in order to verify the correctness of the calculation method, numerical simulation of the natural convection in a triangular cavity containing a circular heat generator is carried out by using the algorithm adopted in the paper, and the obtained results of the calculation of the average Nusselt number of the heat generator are compared with the simulation results of Xu X et al.[13] The obtained results of the average Nusselt number of the heat generator are compared with the simulation results of Xu X et al. It is found that the results obtained by the calculation method used in this paper are in good agreement with those obtained in the literature, which verifies the reasonableness of the calculations in this paper.

Table .2 Comparison of calculation results

D/H	Results of this paper	Literatures	Deviation in per cent
1/6	17.065	17.714	-3.66
1/3	25.972	26.416	-1.68
1/2	33.119	32.286	2.58

5. Results and analyses

5.1. Effect of Rayleigh number and heat generator size on flow and heat transfer

5.1.1. Distribution of isotherms and streamlines

Figure. 2 shows the streamline distribution when the Rayleigh number is 103 to 106 and the heat generator m is 0.1D to 0.4D. It can be seen from the streamline diagram that the air is heated when it is close to the heat generator, moves upward under the action of the buoyancy force, and encounters the cold wall to be cooled and moves downward, thus forming two vortices in the cavity. When Ra=103 and 104, the distribution of the flow lines in the cavity is basically the same and symmetrical about the x-axis and y-axis, which

is because when the Ra number is lower, the main mode of heat transfer in the cavity is thermal conductivity, and the degree of air flow in the cavity is weak. With the increasing of Ra number, when Ra=105 and 106, the main heat transfer mode in the cavity transitions from heat conduction to convection, and the flow of air in the cavity is intensified. The symmetry of the flow lines in the cavity about the y-axis is still good, but the symmetry about the x-axis is broken, the two vortices gradually move upward, and the flow lines directly above the heat generator become denser.

The size of the heat generator mainly affects the flow and heat transfer by changing the size and shape of the space in the cavity, with the increase of m, the heat generator continuously squeezes the space on both sides of the cavity, and the vortex on both sides of the cavity is continuously squeezed and elongated until it is detached.

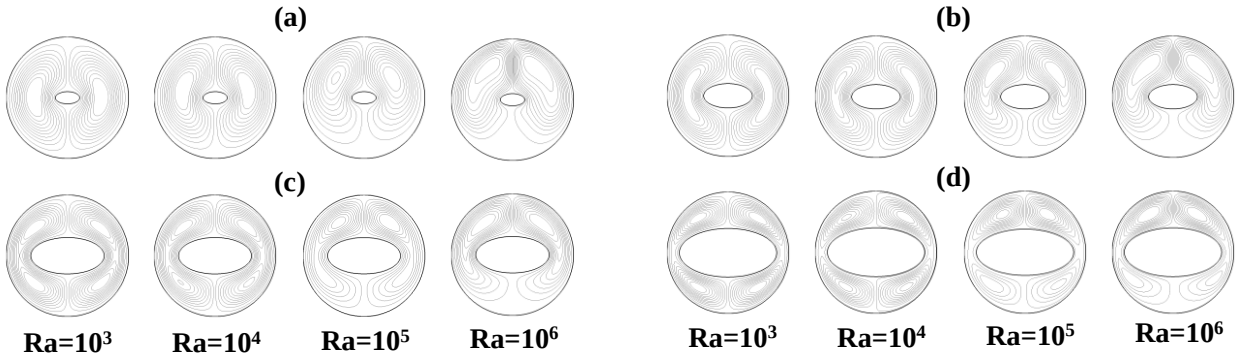

Fig.2 m=0.1D(a), 0.2D(b), 0.3D(c), 0.4D(d) Streamline distribution in the cavity

Figure 3 shows the isothermal distribution when the Rayleigh number is 103 to 106 and the heat generator m is 0.1D to 0.4D. From the isotherms, it can be seen that the isotherms are only around the heat generator, similar to the distribution of flow lines, when Ra = 103 and 104, due to the thermal conductivity as the main mode of heat transfer, the isotherms in the cavity are symmetric about the x-axis and y-axis. When Ra = 105, the degree of convection in the cavity increases, under the action of the buoyancy force, the upper surface of the heating body rises a plume of heat flow, resulting in the isothermal line of the whole upward shift. When Ra=106, the degree of convection in the cavity continues to increase, and the distortion of the isotherm is more obvious. With the increase of m, the isotherms on both sides of the cavity are more intensive.

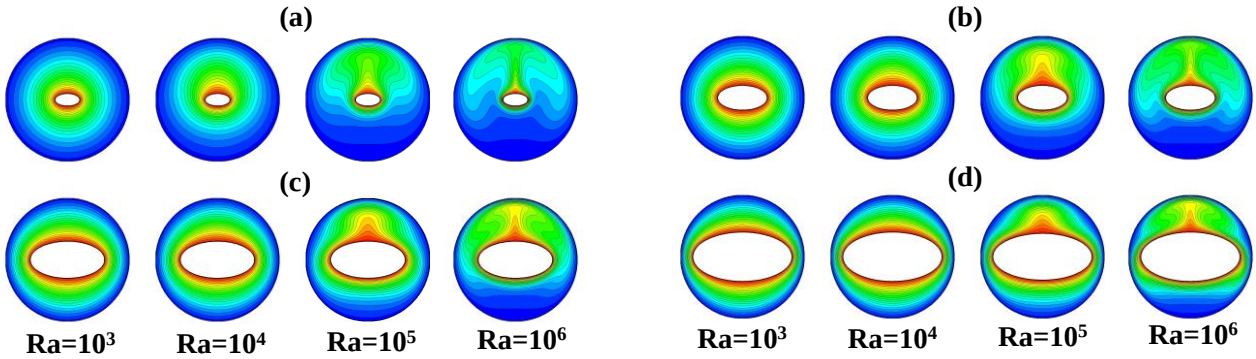

Fig.3 m=0.1D(a), 0.2D(b), 0.3D(c), 0.4D(d) isothermal distribution in the cavity

5.1.2. Partial and average Nusselt numbers

Figure. 4 shows the trend of the local Nusselt number of the surface of the heat generator and the cavity with θ at m=0.1D(a), 0.2D(b), 0.3D(c), and 0.4D(d). From Figure. 4(a) and (b), it can be seen that the distributions of Nusselt numbers on the surface of the heat generator and the cavity are similar at different Rayleigh numbers when the heat generator m=0.1D and 0.2D, which is due to the small size of the heat generator relative to the cavity and the small influence caused by the geometry on the air flow in the cavity.

For the heater, there are local minima in the surface local Nusselt number around θ=90° and θ=270° , and local maxima around θ=0° and θ=180° . At Rayleigh numbers of 103 and 104, the values of the surface localized Nusselt number are closer to each other due to the weaker convection in the cavity. When the Rayleigh number is 105 and 106, the degree of convection in the cavity is intensified, and the variation of the surface Nusselt number increases, especially in the upper part of the heat generator, because according to Figure. 3, when the Rayleigh number is 105 and 106, the plume of heat flow rising from the centre of the upper surface of the heat generator collides with the cavity wall, and the air flow in the upper part of the cavity is more intense, resulting in a more significant variation of the Nusselt number of this part of the chamber; however, due to the rising of the plume of rising heat flow, the temperature of the upper part of the cavity is significantly higher than that of the lower part, so that the temperature difference between the upper surface of the heat generating body and the air is smaller than the temperature difference between the lower surface and the air, and the value of the local Nusselt number of the upper surface of the heat generating body is also smaller than that of the lower surface.

For the cavity, for Rayleigh numbers of 103 and 104, the surface Nusselt number is basically a horizontal line, because the convection in the cavity is very weak at this time. Rayleigh number of 105 , 106 , the surface of the local Nusselt

number at θ=90°there is a very small value, in the vicinity of θ=270° there is a very large value, and in the vicinity of θ=270° the magnitude of change is more intense, the reason is also the rise of the plume of heat generator and the cavity generated by the collision of the plume of heat flow; the lower surface of the lower surface of the cavity of the local Nusselt number is lower than the upper surface, which is due to the lower part of the cavity body temperature is lower than the upper part of the cavity body, resulting in a larger low-temperature zone, the lower part of the chamber, the temperature is very low, and the temperature is lower than the upper part of the chamber. The temperature difference between the lower wall of the cavity and the air is very small, so the local Nusselt number on the lower surface of the cavity is lower than that on the upper.

When the heat generator m=0.3D, the trend of Nusselt number distribution between the surface of the heat generator and the surface of the cavity (Figure. 4c) is similar to that of Fig. a Fig. b. However, with the gradual increase of the heat generator, it produces a certain change in the fluid region inside the cavity. The main change occurs at Ra=105, from the curve, the local Nusselt number of the surface of the heat generator and the cavity is closer to Ra=103 and 104, which indicates that the increase of the heat generator makes the volume of the air domains on both sides of the cavity compressed, thus reducing the intensity of convective heat transfer.

When the heater m=0.4D (Figure. 4d), the main heat transfer mode in the cavity is convection, and the air flow in the cavity is more irregular, the local Nusselt number between the surface of the heater and the cavity produces a larger change. The local Nusselt number of the heater is greatly increased on both sides of the heater at Ra=103 and 104, which is caused by the gap between the two sides of the heater and the cavity due to the geometry. This is caused by the smaller gap between the two sides of the heater and the cavity due to the geometry. At Ra=105, the surface local Nusselt number of the heater changes more drastically, but the distribution trend remains the same; the cavity surface local Nusselt number has very large values near θ=180°and θ=270°, and very small values near θ=195°and θ=330°. At Ra=106 , the local Nusselt number on the surface of the heat generator has very small values near θ=15°, θ=165° , θ=270° and very large values near θ=210° and θ=330° ; the local Nusselt number on the surface of the cavity has very small values near θ=15° , θ=165° , θ=270° and very large values near θ=90° , θ=195° and θ=345° , which is mainly due to strong convection due to buoyancy.

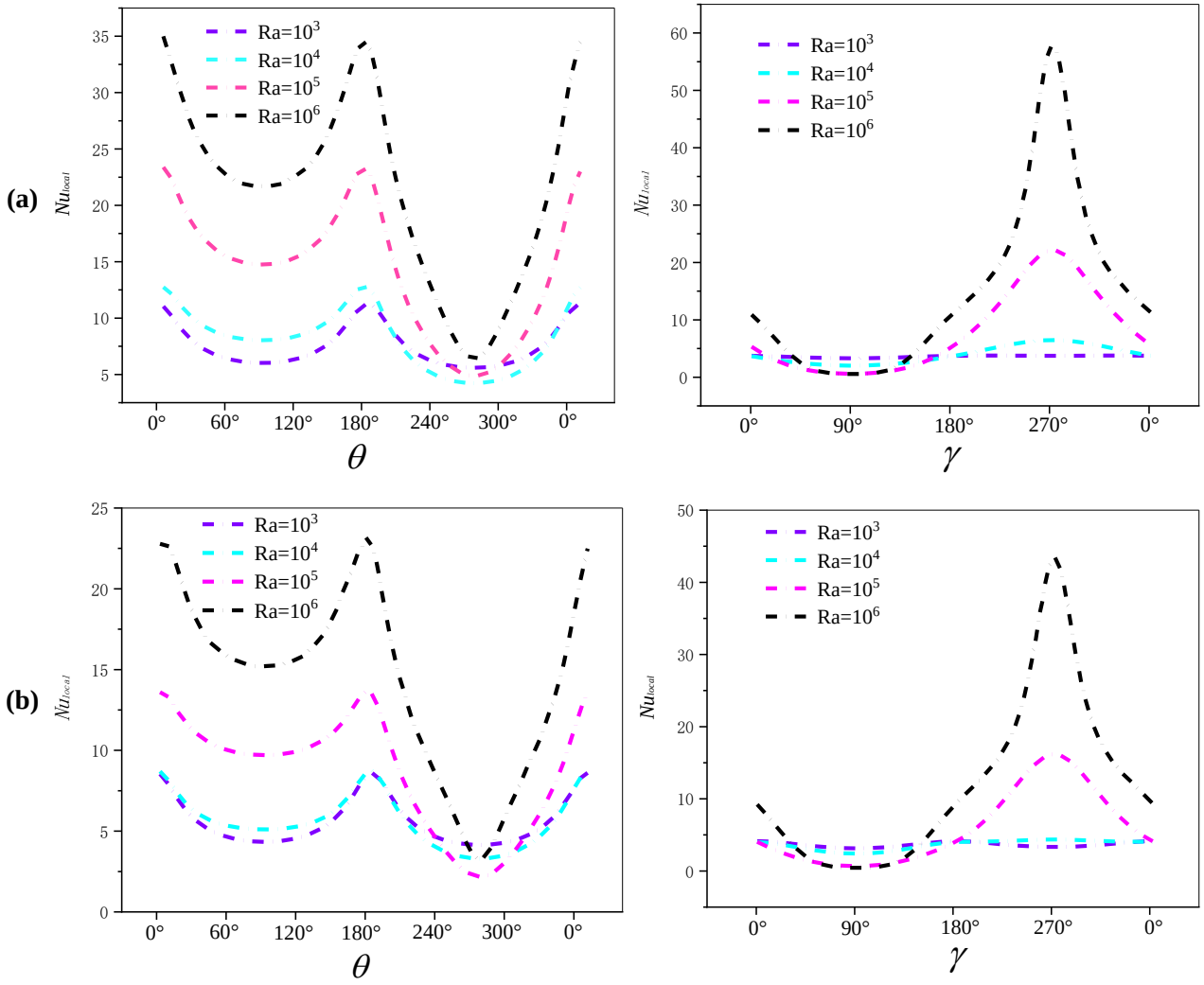

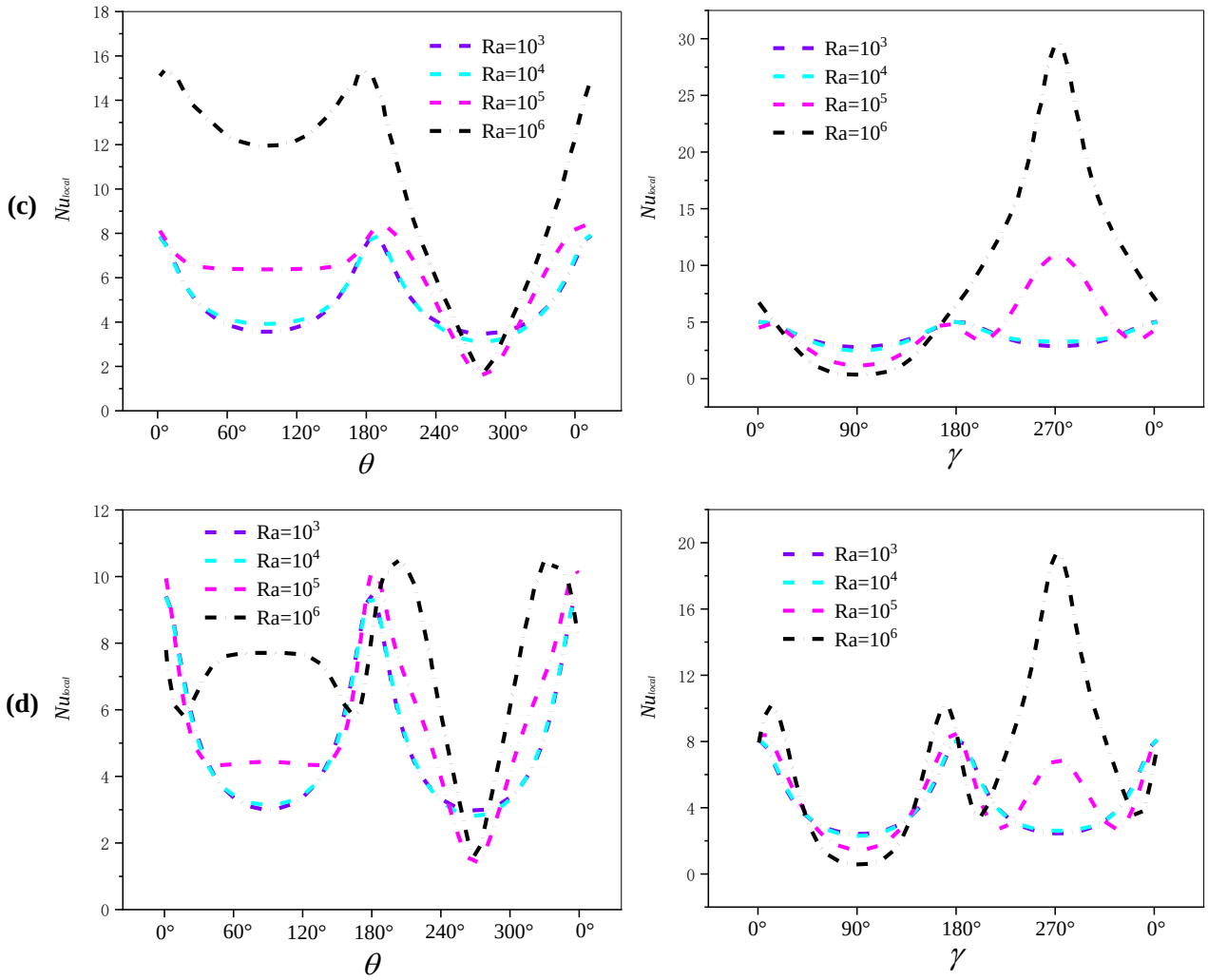

Fig.4 m=0.1D(a), 0.2D(b), 0.3D(c), 0.4D(d) variation trend of heater(left) and cavity(right) local Nusselt number with θ

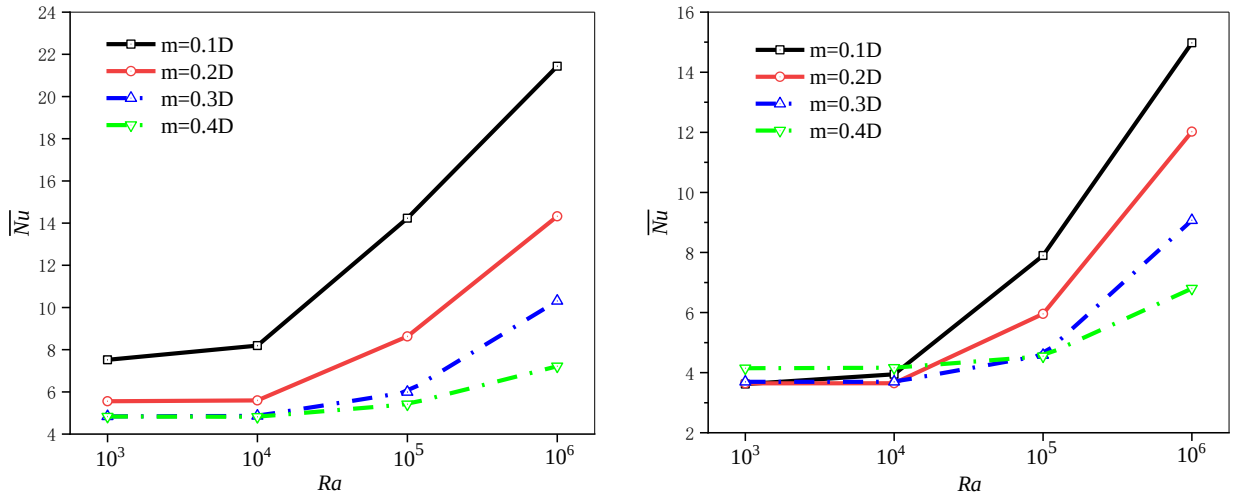

Fig.5 The trend of average Nusselt number variation between the heating body and cavity surface under different Rayleigh numbers

Figure 5 gives the trend of the average Nusselt number between the heat generator and the cavity surface at different Rayleigh numbers. It can be seen from the figure, Ra = 103 and 104 when the average Nusselt number of the heat generator and the cavity surface is relatively close, because the degree of convection at this time is very weak; with the increase of Ra, the average Nusselt number of the heat generator and the cavity surface increase; with the increase of m, the average Nusselt number of the heat generator and the cavity surface are decreased; this indicates that the size of the heat generator and the Rayleigh number of the natural convection inside the cavity to play the opposite effect As the Rayleigh number increases, the stronger the degree of convection in the cavity, and as the heating body m increases, the space in the cavity is compressed, and the strength of natural convection is weakened, which is more unfavorable to the heat dissipation in the cavity.

5.2. Effect of heat source rotation angle on heat transfer and flow

Figure 6 shows the distribution of isotherms and streamlines in the cavity at different rotation angles of the heat generator at Ra=105, from which it can be seen that the rotation angle of the heat generator has a certain influence on the distribution of isotherms and streamlines in the cavity. When φ=30°, the rising plume of heat flow from the center of the upper surface of the heat generator is shifted to the right to a certain extent, and the vortex in the upper part of the flow line separates at the upper tip of the heat generator, and a smaller vortex is detached in the upper part of the cavity. When φ=60° , the position of the rising heat flow of the heat generating body is shifted to the upper part and is mainly concentrated on the right side, while the flow line creates two more uniform vortices on both sides of the heat generating body. When φ=90° , the surface heat flow of the heat generator is uniformly distributed at the upper tip, and the two vortices of the flow line are symmetrically distributed in the cavity.

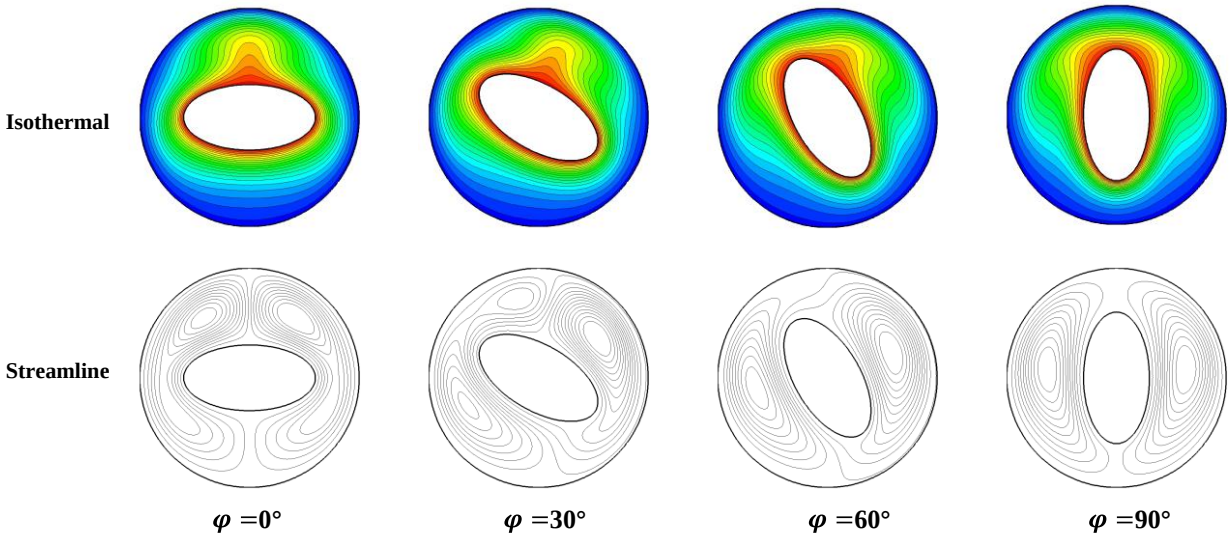

Fig 6 Distribution of isothermal and streamlines in the cavity at different rotation angle

The distribution of local and average Nusselt numbers on the surface of the heat generator and the cavity is shown in Figure. 7. From Figure. 7(left), it can be seen that the distribution trend of the local Nusselt numbers on the surface of the heat generator with different rotation angles is basically the same. With the increase of the rotation angle, the local peak value near the location gradually increases, and the location of the local minimum value near the location gradually moves away from 270°, which is mainly due to the strong convection effect and

The rotation of the heat generator caused the air flow in the cavity to be affected. The distribution of the local Nusselt number on the cavity surface is shown in Figure. 7(right), which is similar to that of the heat generator, and the overall distribution trend is consistent, and the location and size of its local peaks are shifted and changed with the increase of the rotation angle.

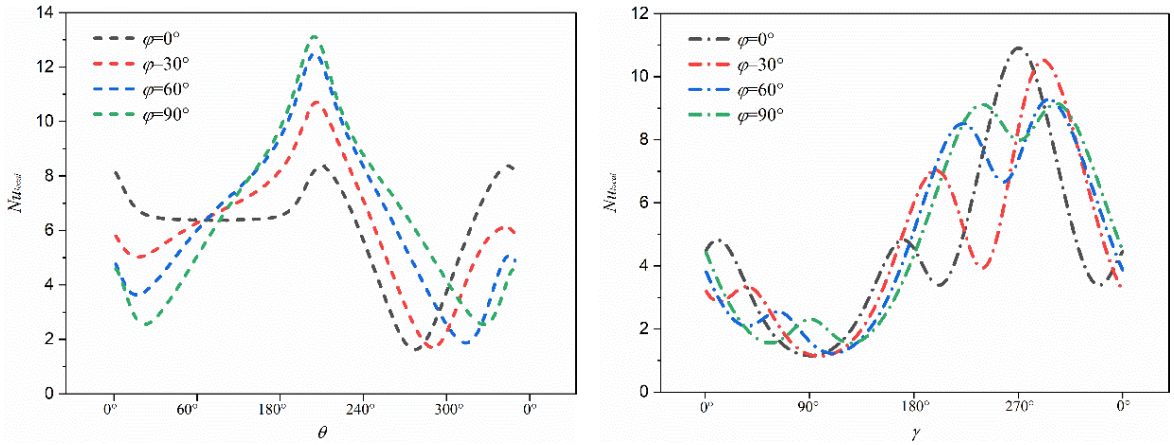

Fig 7 Variation trend of heater(left) and cavity(right) local Nusselt number at different rotation angle

6. Conclusion

(1) With the increase of Rayleigh number, the intensity of natural convection in the cavity gradually increases, and the change of the intensity of natural convection has a great influence on the distribution of isotherms and streamlines in the cavity, and the larger the Rayleigh number is, the more significant the influence is.

(2) Analyze the heat exchange capacity between the heater and the cavity at different Rayleigh numbers, and find that with the increase of Rayleigh number, the natural convection intensity in the cavity gradually increases, the stronger the heat exchange capacity between the heat generator and the cavity, and the Rayleigh number is bigger, and the magnitude

of increase is more drastic.

(3) Comparison of the heat transfer capacity between the surface of the heater and the cavity at different sizes of the heater, it is found that the smaller the heater, the stronger the heat exchange capacity between the heater and the cavity.

(4) Comparison of the heat transfer capacity of the surface of the heat generator and the cavity at different rotation angles of the heater, it is found that the heat transfer capacity of both the heat generator and the cavity is enhanced with the increase of the rotation angle.

Acknowledgements

Luzhou Science and Technology Program (2022-JYJ-165).

References

[1] Song S, Guo X Y. Boussinesq approximation and numerical simulation of natural convection in closed cavities[J]. Mechanics Quarterly. 2012, 33(1): 60-67.

[2] Huang J C, Li G Z, Jiang L X. Numerical study on the transition layer of laminar natural convection heat transfer in a closed cavity[J]. Journal of Huazhong University of Science and Technology. 2001(5): 51-53.

[3] Yang X, Tao W Q Numerical simulation of natural convection in a closed cavity at high Rayleigh number[J]. Journal of Xi'an Jiaotong University. 2014, 48(5): 27-31.

[4] Yang W, Chang J G, Lu Y F, et al. Influence of physical property parameters on numerical simulation of natural convection in closed cavities[J]. Journal of Sichuan University (Natural Science Edition). 2013, 50(3): 566-570.

[5] Sasmal C, Gupta A K, Chhabra R P. Natural convection heat transfer in a power-law fluid from a heated rotating cylinder in a square duct[J]. INTERNATIONAL JOURNAL OF HEAT AND MASS TRANSFER. 2019, 129: 975-996.

[6] Park Y G, Ha M Y, Park J. Natural convection in a square enclosure with four circular cylinders positioned at different rectangular locations[J]. International Journal of Heat & Mass Transfer. 2015, 81: 490-511.

[7] Yong G P, Man Y H, Choi C, et al. Natural convection in a square enclosure with two inner circular cylinders positioned at different vertical locations[J]. International Journal of Heat & Mass Transfer. 2014, 77(4): 501-518.

[8] Yoon H S, Yu D H, Ha M Y, et al. Three-dimensional natural convection in an enclosure with a sphere at different vertical locations[J]. International Journal of Heat & Mass Transfer. 2010, 53(15-16): 3143-3155.

[9] Shen Z J, Yu B. Numerical study of natural convection in hot and cold circular tubes at different vertical positions in a closed square cavity[J]. Chemical Progress. 2015, 34(6): 1595-1601.

[10] Liao C C, Lin C A. Influences of a confined elliptic cylinder at different aspect ratios and inclinations on the laminar natural and mixed convection flows[J]. International Journal of Heat & Mass Transfer. 2012, 55(23-24): 6638-6650.

[11] Ping Z, Zhang X, Deng J, et al. A numerical study of natural convection in an inclined square enclosure with an elliptic cylinder using variational multiscale element free Galerkin method[J]. International Journal of Heat & Mass Transfer. 2016, 99: 721-737.

[12] Wang R, Gao C. Numerical simulation of natural convection in a triangular cavity containing a heat-generating body[J]. Journal of Hefei University of Technology (Natural Science Edition). 2016, 39(2): 161-165.

[13] Xu X, Yu Z, Hu Y, et al. A numerical study of laminar natural convective heat transfer around a horizontal cylinder inside a concentric air-filled triangular enclosure[J]. International Journal of Heat & Mass Transfer. 2010, 53(1): 345-355.